CELL CYCLE, 2018
VOL. 17, NO. 6, 801–809
https://doi.org/10.1080/15384101.2018.1431596

Taylor & Francis
Taylor & Francis Group

REPORT

Tumor-targeting Salmonella typhimurium A1-R combined with recombinant methioninase and cisplatinum eradicates an osteosarcoma cisplatinum-resistant lung metastasis in a patient-derived orthotopic xenograft (PDOX) mouse model: decoy, trap and kill chemotherapy moves toward the clinic

Kentaro Igarashi[a,b,c], Kei Kawaguchi[a,b], Tasuku Kiyuna[a,b], Kentaro Miyake[a,b], Masuyo Miyake[a,b], Shukuan Li[a], Qinghong Han[a], Yuying Tan[a], Ming Zhao[a], Yunfeng Li[d], Scott D. Nelson[d], Sarah M. Dry[d], Arun S. Singh[e], Irmina A. Elliott[f], Tara A. Russell[f], Mark A. Eckardt[g], Norio Yamamoto[c], Katsuhiro Hayashi[c], Hiroaki Kimura[c], Shinji Miwa[c], Hiroyuki Tsuchiya[c], Fritz C. Eilber[f] and Robert M. Hoffman[a,b]

[a]AntiCancer, Inc., San Diego, CA, USA; [b]Department of Surgery, University of California, San Diego, CA, USA; [c]Department of Orthopaedic Surgery, Kanazawa University, Kanazawa, Japan; [d]Dept. of Pathology, University of California, Los Angeles, CA, USA; [e]Division of Hematology-Oncology, University of California, Los Angeles, CA, USA; [f]Division of Surgical Oncology, University of California, Los Angeles, CA, USA; [g]Department of Surgery, Yale School of Medicine, New Haven, CT, USA

ABSTRACT

In the present study, a patient-derived orthotopic xenograft (PDOX) model of recurrent cisplatinum (CDDP)-resistant metastatic osteosarcoma was treated with *Salmonella typhimurium* A1-R (*S. typhimurium* A1-R), which decoys chemoresistant quiescent cancer cells to cycle, and recombinant methioninase (rMETase), which selectively traps cancer cells in late S/G_2, and chemotherapy. The PDOX models were randomized into the following groups 14 days after implantation: G1, control without treatment; G2, CDDP (6 mg/kg, intraperitoneal (i.p.) injection, weekly, for 2 weeks); G3, rMETase (100 unit/mouse, i.p., daily, for 2 weeks). G4, *S. typhimurium* A1-R (5×10^7 CFU/100 μl, i.v., weekly, for 2 weeks); G5, *S. typhimurium* A1-R (5×10^7 CFU/100 μl, i.v., weekly, for 2 weeks) combined with rMETase (100 unit/mouse, i.p., daily, for 2 weeks); G6, *S. typhimurium* A1-R (5×10^7 CFU/100 μl, i.v., weekly, for 2 weeks) combined with rMETase (100 unit/mouse, i.p., daily, for 2 weeks) and CDDP (6 mg/kg, i.p. injection, weekly, for 2 weeks). On day 14 after initiation, all treatments except CDDP alone, significantly inhibited tumor growth compared to untreated control: (CDDP: p = 0.586; rMETase: p = 0.002; *S. typhimurium* A1-R: p = 0.002; *S. typhimurium* A1-R combined with rMETase: p = 0.0004; rMETase combined with both *S. typhimurium* A1-R and CDDP: p = 0.0001). The decoy, trap and kill combination of *S. typhimurium* A1-R, rMETase and CDDP was the most effective of all therapies and was able to eradicate the metastatic osteosarcoma PDOX.

ARTICLE HISTORY
Received 16 October 2017
Accepted 17 January 2018

KEYWORDS
osteosarcoma; metastasis; lung; PDOX; resistance; *Salmonella typhimurium* A1-R; decoy; methioninase; trap; cisplatinum; kill

Introduction

Metastatic osteosarcoma is a recalcitrant disease with a less than 20% long-term survival rate which has not improved for many years [1–7].

In order to develop precision individualized therapy for metastatic ostesosarcoma, we previously established a patient-derived orthotopic xenogrraft (PDOX) of a lung-metastasis from an osteosarcoma of a patient who failed CDDP therapy. Temozolomide (TEM) and trabectedin (TRAB), but not CDDP, significantly inhibited tumor volume compared to untreated control in the PDOX model. This osteosarcoma PDOX model identified potentially, highly-effective drugs for this recalcitrant disease, while accurately maintaining the CDDP resistance of the tumor in the patient [8].

We also previously reported that a subcutaneous mouse model of this CDDP-resistant ostoeosarcoma was sensitive to tumor-targeting *Salmonella typhimurium* A1-R (*S. typhimurium* A1-R) [9].

We also previously showed recombinant methioninase (rMETase) effectively reduced tumor growth of a PDOX model of Ewing's sarcoma compared to untreated control. The methionine level both of plasma and supernatants derived from sonicated tumors was lower in the rMETase group [10].

Tumor-targeting *S. typhimurium* A1-R decoyed chemo-resistant quiescent cancer cells in tumors to cycle from G_0/G_1 to S/G_2/M. When the cancer cells were subsequently treated with rMETase, they were selectively trapped in S/G_2. We showed using sequential treatment of tumors in vivo with *S. typhimurium* A1-R to decoy quiescent cancer cells to cycle and rMETase to selectively trap the decoyed cancer cells in S/G_2 phase, that chemotherapy could eradicate tumors in

CONTACT Hiroyuki Tsuchiya tsuchi@med.kanazawa-u.ac.jp Dept. of Orthopaedic Surgery, Graduate School of Medicine, Kanazawa University, 13-1 Takara-machi, Kanazawa 920–8641, Japan; Fritz C. Eilber fceilber@mednet.ucla.edu Professor of Surgery, Professor of Molecular & Medical Pharmacology, UCLA, Division of Surgical Oncology, 10833 LeConte Avenue, Rm. 54–140 CHS, Los Angeles, CA 90095–1782; Robert M. Hoffman all@anticancer.com AntiCancer, Inc., 7917 Ostrow St., San Diego, CA 92111

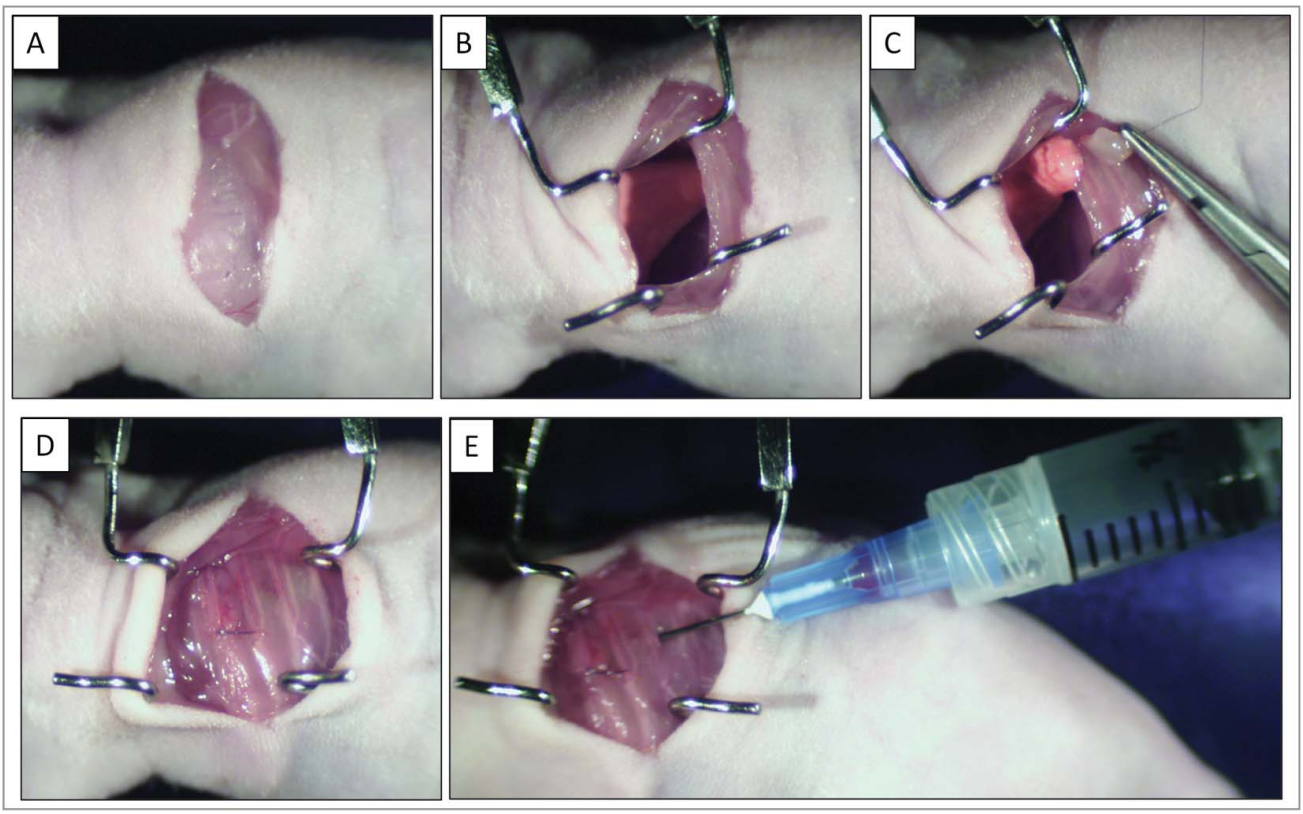

Figure 1. Establishment of osteosarcoma lung metastaswas PDOX model. A) A skin incision was made on the left chest wall. B) Chest muscles were separated and an intercostal incision in the chest wall was made, and the chest wall was opened. C) The left lung was taken up and tumor fragments were sewn into the lower lung with one suture. D) The incision in the chest wall was closed with a 6-0 surgical suture. E) An intrathoracic puncture was made to withdraw the remaining air in the chest cavity.

mouse models of human stomach cancer. These results demonstrated a new praradigm of "decoy, trap and shoot (kill)" chemotherapy [11].

In the present study, we show that sequential treatment of the chemotherapy-resistant osteosarcoma lung metastasis in a PDOX mouse model with *S. typhimurium* A1-R, rMETase and CDDP could eradicate the tumor.

Results and discussion

Sequential treatment of the chemotherapy-resistant osteosarcoma lung metastasis PDOX mouse model with S. typhimurium *A1-R, rMETase and CDDP*

All treatments but CDDP significantly inhibited tumor growth compared to the untreated control on day 14 after initiation

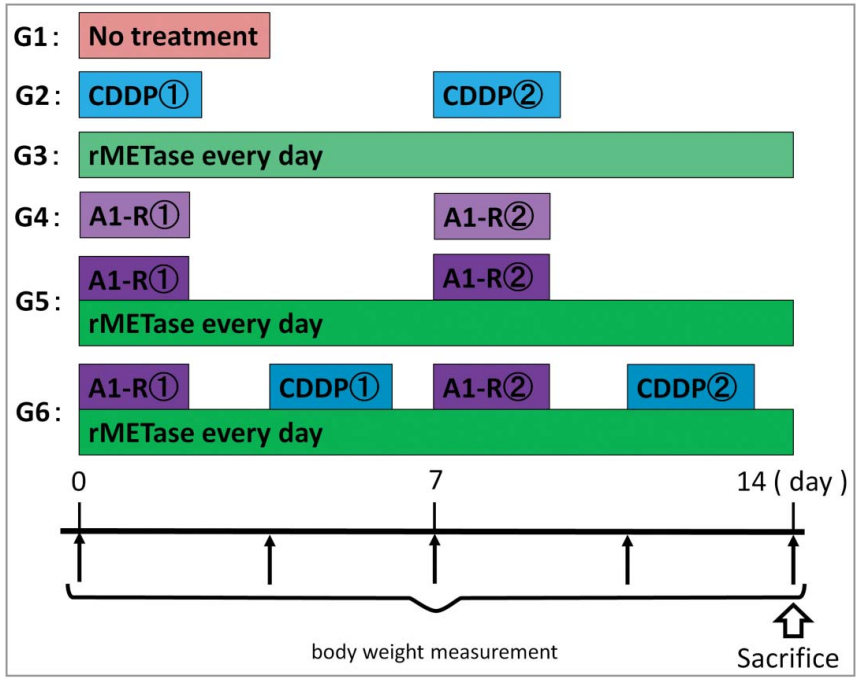

Figure 2. Treatment schema.

(Figures 1 and 2). Tumor volume at day 14 were the following: control (G1): 201±91 mm^3; CDDP (G2): 174±108 mm^3; rMETase (G3): 79±41 mm^3; *S. typhimurium* A1-R (G4): 74±18 mm^3; *S. typhimurium* A1-R+ rMETase (G5) 44±15 mm^3; *S. typhimurium* A1-R+rMETase+CDDP (G6) 15±8 mm^3. Control vs. CDDP (p = 0.586); control vs. rMETase (p = 0.002); control vs. *S. typhimurium* A1-R (p = 0.002); control vs. *S. typhimurium* A1-R+rMETase (p = 0.0004); control vs. *S. typhimurium* A1-R+rMETase+CDDP (p = 0.0001); CDDP vs. rMETase (p = 0.045); CDDP vs. *S. typhimurium* A1-R (p = 0.033); CDDP vs. *S. typhimurium* A1-R+rMETase (p = 0.011); CDDP vs. *S. typhimurium* A1-R+rMETase+CDDP (p = 0.004); rMETase vs. *S. typhimurium* A1-R (p = 0.719); rMETase vs. *S. typhimurium* A1-R+rMETase (p = 0.048); rMETase vs. *S. typhimurium* A1-R+rMETase+CDDP (p = 0.003); *S. typhimurium* A1-R vs. *S. typhimurium* A1-R+rMETase (p = 0.003); *S. typhimurium* A1-R vs. *S. typhimurium* A1-R+rMETase +CDDP (p<0.0001); *S. typhimurium* A1-R+rMETase vs. *S. typhimurium* A1-R+rMETase+CDDP (p = 0.0004) (Figures 3 and 4). There were no animal deaths in any group. The body weight of treated mice was not significantly different in any group (Figure 5).

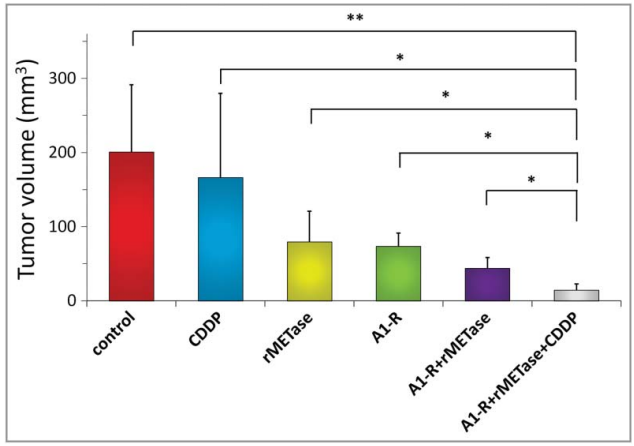

Figure 3. Quantitative in vivo antitumor efficacy of monotherapy of CDDP, rMETase, *S. typhimurium* A1-R, *S. typhimurium* A1-R + rMETase and *S. typhimurium* A1-R + rMETase + CDDP on the lung metastatic osteosarcoma PDOX. Please see Figure 2 for treatment schema. Tumor volume was measured at day 14 at necropsy. N = 8 mice/group. *p<0.005, **p<0.001

Histology of the original tumor and implanted tumors

High power microscopy of the original patient tumor showed neoplastic chondroid matrix occupied by anaplastic cells. The tumor had hypercellular areas populated by anaplastic cells displaying nuclear pleomorphism, coarse and hyperchromatic chromatin and abundant mitotic figures (Figure 6A). High power microscopy of the untreated PDOX tumor showed solid and chondroblastic appearance similar to the patient original tumor with hypercellular areas filled with tumor cells displaying nuclear pleomorphism and mitotic figures (Figure 6B). The PDOX tumor treated with CDDP comprised viable cells without apparent necrosis or inflammatory changes and similar features compared to the untreated control (Figure 6C). The rMETase-treated tumor and *S. typhimurium* A1-R-treated tumor showed changes in sarcoma-cell shapes (Figure 6D and 6E). *S. typhimurium* A1-R combined with rMETase-treated tumor showed reduced cellularity (Figure 6F). The tumor treated with *S. typhimurium* A1-R combined with both rMETase and CDDP showed reduced cellularity and tumor necrosis (Figure 6G) [8].

The present study was made possible by the use of a PDOX model which closely mimics the patient. Toward this goal, our laboratory pioneered the patient-derived orthotopic xenograft (PDOX) nude mouse model with the technique of surgical orthotopic implantation (SOI), including breast [12], ovarian [13], lung [14], cervical [15,16], colon [17–19], stomach [20], pancreatic [21–25], melanoma [26–30], and sarcoma [31–40].

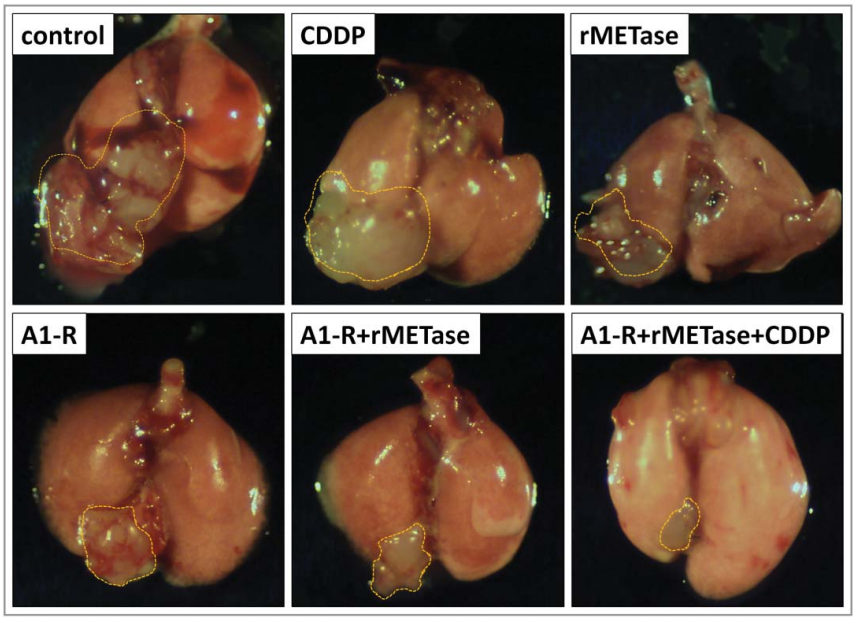

Figure 4. Representative photos of treated and untreated osteosarcoma lung-metastatic PDOX models.

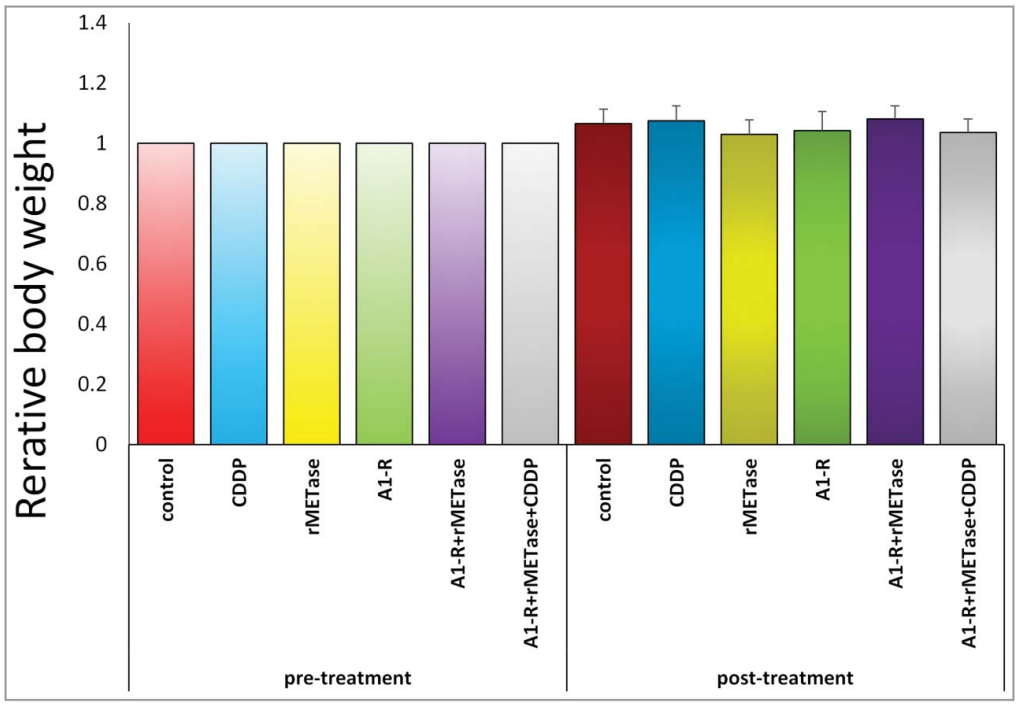

Figure 5. Effect of treatments on osteosarcoma lung metastasis PDOX on mouse body weight. Bar graph shows relative body weight in each treatment group at pre- and post-treatment relative to initial body weight. There were no significant differences between any of the treatment groups or the untreated groups.

The PDOX model, developed by our laboratory over the past 30 years, has many advantages over subcutaneous-transplant models which are growing ectopically under the skin [41]. The PDOX model enables precise, individualized therapy, especially for recalcitrant diseases, for example, metastatic melanoma [26–30] or sarcoma [31–40] by matching the patient tumor to an effective drug identified with the PDOX models.

S. typhimurium A1-R may be a general therapeutic for cancer. *S. typhimurium* A1-R is auxotrophic for Leu–Arg, which prevents it from mounting a continuous infection in normal tissues. *S. typhimurium* A1-R inhibited or eradicate primary and metastatic tumors as monotherapy in nude-mouse models of major cancers [42], including prostate [43,44], breast [45–47], lung [48,49], pancreatic [23,50–53], ovarian [54,55], stomach [56], cervical cancer [57], glioma [58,59], as well as sarcoma [32,60], including osteosarcoma [61–63], all of which are highly aggressive tumor models.

rMETase may also be a general therapeutic for cancer since methionine dependence appears to be a general metabolic defect in cancer [11,64–77].

Previously-developed concepts and strategies of highly-selective tumor targeting can take advantage of molecular targeting of tumors, including tissue-selective therapy which focuses on unique differences between normal and tumor tissues [78–83].

Materials and methods

Animal care

Athymic nu/nu nude mice (AntiCancer Inc., San Diego, CA), 4–6 weeks old, were used in this study. Animals were housed in a barrier facility on a high efficiency particulate arrestance (HEPA)-filtered rack under standard conditions of 12-hour light/dark cycles. The animals were fed an autoclaved laboratory rodent diet. All animal studies were conducted with an AntiCancer Institutional Animal Care and Use Committee (IACUC)-protocol specifically approved for this study and in accordance with the principles and procedures outlined in the National Institute of Health Guide for the Care and Use of Animals under Assurance Number A3873-1. In order to minimize any suffering of the animals, anesthesia and analgesics were used for all surgical experiments. Animals were anesthetized by subcutaneous injection of a 0.02 ml solution of 20 mg/kg ketamine, 15.2 mg/kg xylazine, and 0.48 mg/kg acepromazine maleate. The response of animals during surgery was monitored to ensure adequate depth of anesthesia. The animals were observed on a daily basis and humanely sacrificed by CO_2 inhalation when they met the following humane endpoint criteria: severe tumor burden (more than 20 mm in diameter), prostration, significant body weight loss, difficulty breathing, rotational motion and body temperature drop [8].

Patient-derived tumor

The study was previously reviewed and approved by the UCLA Institutional Review Board (IRB #10-001857) before the study began. Written informed consent was previously obtained from the patient as part of the above-mentioned UCLA Institutional Review Board-approved protocol. A 16-year old patient with localized left distal femoral high grade osteosarcoma previously underwent CDDP based neoadjuvant chemotherapy and limb salvage with distal femoral replacement. The tumor necrosis rate of the primary tumor after cisplatin based chemotherapy was 70%. One year later, the osteosarcoma relapsed with three bilateral metachronous pulmonary metastases. The patient was

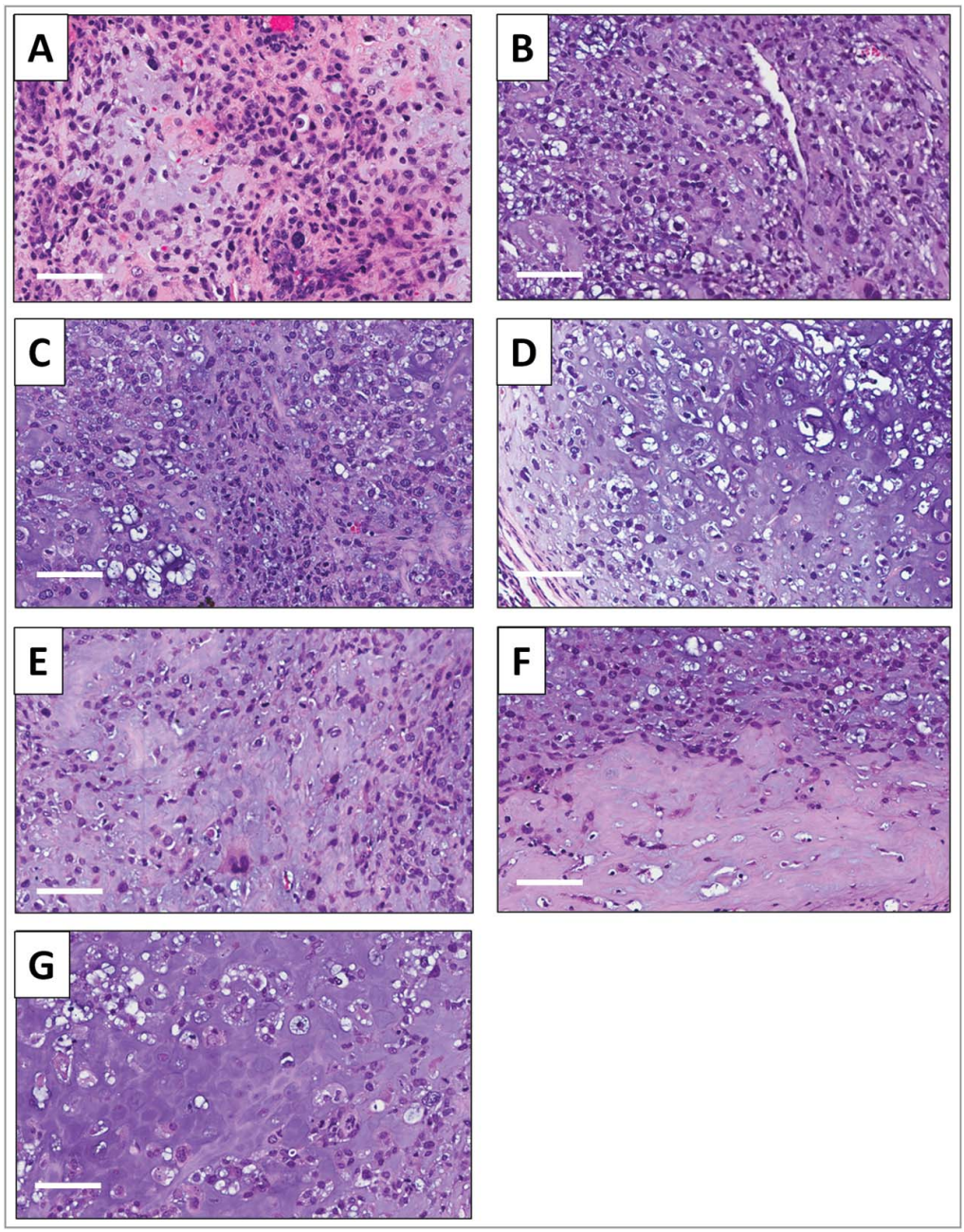

Figure 6. Effect of treatment on osteosarcoma lung metastasis PDOX tumor histology. A) Hematoxylin and eosin (H&E)-stained section of the original patient lung metastasis. B) Untreated PDOX tumor. C) PDOX tumor treated with CDDP. D) PDOX tumor treated with rMETase. E) PDOX tumor treated with *S. typhimurium* A1-R. F) PDOX tumor treated with *S. typhimurium* A1-R combined with rMETase and G) PDOX tumor treated with *S. typhimurium* A1-R combined with both rMETase and CDDP. White scale bars: 80μm.

treated with curative surgery at the Division of Surgical Oncology, University of California, Los Angeles (UCLA). The patient did not receive chemotherapy or radiotherapy prior to lung surgery [8].

Surgical orthotopic implantation (SOI) for establishment of PDOX model

The previously established osteosarcoma PDOX was further established in the lung of nude mice in a previous study [8]. After anesthesia, mice are put in a position of right lateral decubitus, with four limbs restrained. A 1.5 cm transverse incision of the skin was made in the left chest wall. Chest muscles were separated by sharp dissection and costal and intercostal muscles were exposed. A 0.8-1.0 cm intercostal incision between the sixth and seventh rib on the chest wall was made, and the chest wall was opened. The left lung was taken up with a forceps, and tumor fragments were sewn promptly into the lower lung with one suture. The lung was then returned into the chest cavity. The incision in the chest wall was closed by a 6-0 surgical suture (Ethilon, Ethicon, Inc., NJ, USA). The closed condition of the chest walls examined immediately, and if a leak existed, it was closed by additional sutures. After closing the chest wall, an intrathoracic puncture was made by using a 3-ml syringe and 25G 1/2 needle to withdraw the remaining air in the chest cavity. After the withdrawal of air, a completely

inflated lung could be seen through the thin chest wall of the mouse. Then the skin and chest muscle were closed with a 6-0 surgical suture in one layer (Figure 1) [14].

Preparation and administration of S. typhimurium A1-R

GFP-expressing *S. typhimurium* A1-R (AntiCancer Inc.) were grown overnight on LB medium (Fisher Sci., Hanover Park, IL, USA) and then diluted 1:10 in LB medium. Bacteria were harvested at late-log phase, washed with PBS, and then diluted in PBS. For an intra-venous injection, a total of 5×10^7 CFU *S. typhimurium* A1-R in 100 μl PBS was administered to each mouse [43–45].

rMETase production

The pAC-1 rMETase high expression clone was used for rMETase production. The fermentation procedure for host E.coli cells and the purification protocol for rMETase were the same as previously described: rMETase was purified by 3 different steps using columns of DEAE Sepharose FF and Sephacryl S-200HR, and ActiClean Etox, which is designed for eliminating endotoxin [77].

Treatment study design

The osteosaroma PDOX lung-metastasis models were randomized into the following groups 14 days after implantation (Figures 1 and 2): G1, control without treatment; G2, CDDP (6 mg/kg, intraperitoneal (i.p.) injection, weekly, for 2 weeks); G3, rMETase (100 unit/mouse, i.p., daily, for 2 weeks). G4, *S. typhimurium* A1-R (5×10^7 CFU/100 μl, i.v., weekly, for 2 weeks); G5, *S. typhimurium* A1-R (5×10^7 CFU/100 μl, i.v., weekly, for 2 weeks) combined with rMETase (100 unit/mouse, i.p., daily, for 2 weeks); G6, *S. typhimurium* A1-R (5×10^7 CFU/100 μl, i.v., weekly, for 2 weeks) combined with rMETase (100 unit/mouse, i.p., daily, for 2 weeks) and CDDP (6 mg/kg, i.p. injection, weekly, for 2 weeks) (Figure 2). Body weight was measured with a digital balance twice a week. 14 days after initiation of treatment, all mice were sacrificed and tumors in the lung were assessed. Tumor volume was calculated by following formula: Tumor volume (mm^3) = length (mm) $\times$ width (mm) $\times$ width (mm) $\times$ 1/2. Data are presented as mean $\pm$ SD.

Histological examination

Fresh tumor samples were fixed in 10% formalin and embedded in paraffin before sectioning and staining. Tissue sections (3 μm) were deparaffinized in xylene and rehydrated in an ethanol series. Hematoxylin and eosin (H&E) staining was performed according to standard protocols. Histological examination was performed with a BHS system microscope. Images were acquired with INFINITY ANALYZE software (Lumenera Corporation, Ottawa, Canada) [8].

Disclosure of potential conflicts of interest

No potential conflicts of interest were disclosed.

Funding

National Cancer Institute (grant number CA213649).

ORCID

Tara A. Russell http://orcid.org/0000-0002-3912-3601
Mark A. Eckardt http://orcid.org/0000-0002-9528-8419
Fritz C. Eilber http://orcid.org/0000-0003-3336-9333

References

[1] Bacci G, Ferrari S, Lari S, et al. Osteosarcoma of the limb: amputation or limb salvage in patients treated by neoadjuvant chemotherapy. J Bone Joint Surg Br. 2002;84:88-92. 10.1302/0301-620X.84B1.12211. PMID:11837839
[2] Muscolo DL, Ayerza MA, Aponte-Tinao LA, et al. Partial epiphyseal preservation and intercalary allograft reconstruction in high-grade metaphyseal osteosarcoma of the knee. J Bone Joint Surg Am. 2004;86:2686-2693. 10.2106/00004623-200412000-00015. PMID:15590854
[3] Simon MA, Aschliman MA, Thomas N, et al. Limb salvage treatment versus amputation for osteosarcoma of the distal end of the femur. J Bone Joint Surg Am. 1986;68:1331-1337. 10.2106/00004623-198668090-00005. PMID:3465732
[4] Lewis VO. What's new in musculoskeletal oncology. J Bone Joint Surg Am. 2007;89:1399-1407. 10.2106/00004623-200706000-00030. PMID:17545444
[5] Meyers PA, Gorlick R, Heller G, et al. Intensification of preoperative chemotherapy for osteogenic sarcoma: results of the Memorial Sloan-Kettering (T-12) protocol. J Clin Oncol. 1998;16:2452-2458. 10.1200/JCO.1998.16.7.2452. PMID:9667263
[6] Fuchs N, Bielack SS, Epler D, et al. Long-term results of the cooperative German-Austrian-Swiss osteosarcoma study group's protocol COSS-86 of intensive multidrug chemotherapy and surgery for osteosarcoma of the limbs. Ann Oncol. 1998;9:893-899. 10.1023/A:1008391103132. PMID:9789613
[7] Bacci G, Briccoli A, Ferrari S, et al. Neoadjuvant chemotherapy for osteosarcoma of the extremity: long-term results of the Rizzoli's 4th protocol. Eur J Cancer. 2001;37:2030-2039. 10.1016/S0959-8049(01)00229-5. PMID:11597381
[8] Igarashi K, Murakami T, Kawaguchi K, et al. A patient-derived orthotopic xenograft (PDOX) mouse model of an cisplatinum-resistant osteosarcoma lung metastasis that was sensitive to temozolomide and trabectedin: implications for precision oncology. Oncotarget. 2017;8:62111-62119. 10.18632/oncotarget.19095. PMID:28977930
[9] Murakami T, Igarashi K, Kawaguchi K, et al. Tumor-targeting Salmonella typhimurium A1-R regresses an osteosarcoma in a patient-derived xenograft model resistant to a molecular-targeting drug. Oncotarget. 2017;8:8035-8042. 10.18632/oncotarget.14040. PMID:28030831
[10] Murakami T, Li S, Han Q, et al. Recombinant methioninase effectively targets a Ewing's sarcoma in a patient-derived orthotopic xenograft (PDOX) nude-mouse model. Oncotarget. 2017;8:35630-35638. 10.18632/oncotarget.15823. PMID:28404944
[11] Yano S, Takehara K, Zhao M, et al. Tumor-specific cell-cycle decoy by Salmonella typhimurium A1-R combined with tumor-selective cell-cycle trap by methioninase overcome tumor intrinsic chemoresistance as visualized by FUCCI imaging. Cell Cycle. 2016;15:1715-1723. 10.1080/15384101.2016.1181240. PMID:27152859
[12] Fu X, Le P, Hoffman RM. A metastatic-orthotopic transplant nude-mouse model of human patient breast cancer. Anticancer Res. 1993;13:901-904. PMID:8352558
[13] Fu X, Hoffman RM. Human ovarian carcinoma metastatic models constructed in nude mice by orthotopic transplantation of histologically-intact patient specimens. Anticancer Res. 1993;13:283-286. PMID:8517640
[14] Wang X, Fu X, Hoffman RM. A new patient-like metastatic model of human lung cancer constructed orthotopically with intact tissue via

thoracotomy in immunodeficient mice. Int J Cancer. 1992;51:992-995. 10.1002/ijc.2910510626. PMID:1639545

[15] Hiroshima Y, Zhang Y, Zhang N, et al. Establishment of a patient-derived orthotopic xenograph (PDOX) model of HER-2-positive cervical cancer expressing the clinical metastatic pattern. PLoS One. 2015;10:e0117417. 10.1371/journal.pone.0117417. PMID:25689852

[16] Murakami T, Kiyuna T, Kawaguchi K, et al. The irony of highly-effective bacterial therapy of a patient-derived orthotopic xenograft (PDOX) model of Ewing's sarcoma, which was blocked by Ewing himself 80 years ago. Cell Cycle. 2017;16:1046-1052. 10.1080/15384101.2017.1304340. PMID:28296559

[17] Hiroshima Y, Maawy A, Metildi CA, et al. Successful fluorescence-guided surgery on human colon cancer patient-derived orthotopic xenograft mouse models using a fluorophore-conjugated anti-CEA antibody and a portable imaging system. J Laparoendosc Adv Surg Tech A. 2014;24:241-247. 10.1089/lap.2013.0418. PMID:24494971

[18] Fu X, Besterman JM, Monosov A, et al. Models of human metastatic colon cancer in nude mice orthotopically constructed by using histologically intact patient specimens. Proc Natl Acad Sci USA. 1991;88:9345-9349. 10.1073/pnas.88.20.9345. PMID:1924398

[19] Metildi CA, Kaushal S, Luiken GA, et al. Fluorescently-labeled chimeric anti-CEA antibody improves detection and resection of human colon cancer in a patient-derived orthotopic xenograft (PDOX) nude mouse model. J Surg Oncol. 2014;109:451-458. 10.1002/jso.23507. PMID:24249594

[20] Furukawa T, Kubota T, Watanabe M, et al. Orthotopic transplantation of histologically intact clinical specimens of stomach cancer to nude mice: correlation of metastatic sites in mouse and individual patient donors. Int J Cancer. 1993;53:608-612. 10.1002/ijc.2910530414. PMID:8436434

[21] Fu X, Guadagni F, Hoffman RM. A metastatic nude-mouse model of human pancreatic cancer constructed orthotopically with histologically intact patient specimens. Proc Natl Acad Sci USA. 1992;89:5645-5649. 10.1073/pnas.89.12.5645. PMID:1608975

[22] Kawaguchi K, Igarashi K, Murakami T, et al. MEK inhibitors cobimetinib and trametinib, regressed a gemcitabine-resistant pancreatic cancer patient-derived orthotopic xenograft (PDOX). Oncotarget. 2017;8:47490-47496. 10.18632/oncotarget.17667. PMID:28537897

[23] Hiroshima Y, Zhang Y, Murakami T, et al. Efficacy of tumor-targeting Salmonella typhimurium A1-R in combination with anti-angiogenesis therapy on a pancreatic cancer patient-derived orthotopic xenograph (PDOX) and cell line mouse models. Oncotarget. 2014;5:12346-12357. 10.18632/oncotarget.2641. PMID:25402324

[24] Hiroshima Y, Maawy A, Zhang Y, et al. Metastatic recurrence in a pancreatic cancer patient derived orthotopic xenograft (PDOX) nude mouse model is inhibited by neoadjuvant chemotherapy in combination with fluorescence-guided surgery with an anti-CA 19–9-conjugated fluorophore. PLoS One. 2014;9:e114310. 10.1371/journal.pone.0114310. PMID:25463150

[25] Hiroshima Y, Maawy AA, Katz MH, et al. Selective efficacy of zoledronic acid on metastasis in a patient-derived orthotopic xenograph (PDOX) nude-mouse model of human pancreatic cancer. J Surg Oncol. 2015;111:311-315. 10.1002/jso.23816. PMID:25394368

[26] Yamamoto M, Zhao M, Hiroshima Y, et al. Efficacy of tumor-targeting Salmonella typhimurium A1-R on a melanoma patient-derived orthotopic xenograft (PDOX) nude-mouse model. PLoS One. 2016;11:e0160882. 10.1371/journal.pone.0160882. PMID:27500926

[27] Kawaguchi K, Murakami T, Chmielowski B, et al. Vemurafenib-resistant BRAF-V600E mutated melanoma is regressed by MEK targeting drug trametinib, but not cobimetinib in a patient-derived orthotopic xenograft (PDOX) mouse model. Oncotarget. 2016;7:71737-71743. PMID:27690220

[28] Kawaguchi K, Igarashi K, Murakami T, et al. Tumor-targeting Salmonella typhimurium A1-R combined with Temozolomide regresses malignant melanoma with a BRAF-V600 mutation in a patient-derived orthotopic xenograft (PDOX) model. Oncotarget. 2016;7:85929-85936. PMID:27835903

[29] Kawaguchi K, Igarashi K, Murakami T, et al. Salmonella typhimurium A1-R targeting of a chemotherapy resistant BRAF-V600E melanoma in a patient-derived orthotopic xenograft (PDOX) model is enhanced in combination with either vemurafenib or temozlomide. Cell Cycle. 2017;16:1288-1294. 10.1080/15384101.2017.1314420. PMID:28622068

[30] Kawaguchi K, Igarashi K, Murakami T, et al. Tumor-targeting Salmonella typhimurium A1-R sensitizes melanoma with a BRAF-V600E mutation to vemurafenib in a patient-derived orthotopic xenograft (PDOX) nude mouse model. J Cell Biochem. 2017;118:2314-2319. 10.1002/jcb.25886. PMID:28106277

[31] Murakami T, Singh AS, Kiyuna T, et al. Effective molecular targeting of CDK4/6 and IGF-1R in a rare FUS-ERG fusion CDKN2A-deletion doxorubicin-resistant Ewing's sarcoma patient-derived orthotopic xenograft (PDOX) nude-mouse model. Oncotarget. 2016;7:47556-47564. 10.18632/oncotarget.9879. PMID:27286459

[32] Murakami T, DeLong J, Eilber FC, et al. Tumor-targeting Salmonella typhimurium A1-R in combination with doxorubicin eradicate soft tissue sarcoma in a patient-derived orthotopic xenograft PDOX model. Oncotarget. 2016;7:12783-12790. 10.18632/oncotarget.7226. PMID:26859573

[33] Murakami T, Li S, Han Q, et al. Recombinant methioninase effectively targets a Ewing's sarcoma in a patient-derived orthotopic xenograft (PDOX) nude-mouse model. Oncotarget. 2017;8:35630-35638. 10.18632/oncotarget.15823. PMID:28404944

[34] Igarashi K, Kawaguchi K, Murakami T, et al. High efficacy of pazopanib on an undifferentiated spindle-cell sarcoma resistant to first-line therapy is identified with a patient-derived orthotopic xenograft (PDOX) nude mouse model. J Cell Biochem. 2017;118:2739-2743. 10.1002/jcb.25923. PMID:28176365

[35] Igarashi K, Kawaguchi K, Kiyuna T, et al. Temozolomide combined with irinotecan caused regression in an adult pleomorphic rhabdomyosarcoma patient-derived orthotopic xenograft (PDOX) nude-mouse model. Oncotarget. 2017;8:75874-75880. 10.18632/oncotarget.16548. PMID:29100276

[36] Igarashi K, Kawaguchi K, Kiyuna T, et al. Patient-derived orthotopic xenograft (PDOX) mouse model of adult rhabdomyosarcoma invades and recurs after resection in contrast to the subcutaneous ectopic model. Cell Cycle. 2017;16:91-94. 10.1080/15384101.2016.1252885. PMID:27830986

[37] Igarashi K, Kawaguchi K, Murakami T, et al. Intra-arterial administration of tumor-targeting Salmonella typhimurium A1-R regresses a cisplatin-resistant relapsed osteosarcoma in a patient-derived orthotopic xenograft (PDOX) mouse model. Cell Cycle. 2017;16:1164-1170. 10.1080/15384101.2017.1317417. PMID:28494180

[38] Hiroshima Y, Zhang Y, Zhang N, et al. Patient-derived orthotopic xenograft (PDOX) nude mouse model of soft-tissue sarcoma more closely mimics the patient behavior in contrast to the subcutaneous ectopic model. Anticancer Res. 2015;35:697-701. PMID:25667448

[39] Kawaguchi K, Igarashi K, Murakami T, et al. Combination of gemcitabine and docetaxel regresses both gastric leiomyosarcoma proliferation and invasion in an imageable patient-derived orthotopic xenograft (iPDOX) model. Cell Cycle. 2017;16:1063-1069. 10.1080/15384101.2017.1314406. PMID:28426279

[40] Kiyuna T, Murakami T, Tome Y, et al. High efficacy of tumor-targeting Salmonella typhimurium A1-R on a doxorubicin- and dactolisib-resistant follicular dendritic-cell sarcoma in a patient-derived orthotopic xenograft PDOX nude mouse model. Oncotarget. 2016;7:33046-33054. 10.18632/oncotarget.8848. PMID:27105519

[41] Hoffman RM. Patient-derived orthotopic xenografts: better mimic of metastasis than subcutaneous xenografts. Nat Rev Cancer. 2015;15:451-452. 10.1038/nrc3972. PMID:26422835

[42] Hoffman RM. Future of bacterial therapy of cancer. Methods Mol Biol. 2016;1409:177-184. 10.1007/978-1-4939-3515-4_15. PMID:26846811

[43] Zhao M, Yang M, Li XM, et al. Tumor-targeting bacterial therapy with amino acid auxotrophs of GFP-expressing Salmonella typhimurium. Proc Natl Acad Sci USA. 2005;102:755-760. 10.1073/pnas.0408422102. PMID:15644448

[44] Zhao M, Geller J, Ma H, et al. Monotherapy with a tumor-targeting mutant of Salmonella typhimurium cures orthotopic metastatic mouse models of human prostate cancer. Proc Natl Acad Sci USA. 2007;104:10170-10174. 10.1073/pnas.0703867104. PMID:17548809
[45] Zhao M, Yang M, Ma H, et al. Targeted therapy with a Salmonella typhimurium leucine-arginine auxotroph cures orthotopic human breast tumors in nude mice. Cancer Res. 2006;66:7647-7652. 10.1158/0008-5472.CAN-06-0716. PMID:16885365
[46] Zhang Y, Tome Y, Suetsugu A, et al. Determination of the optimal route of administration of Salmonella typhimurium A1-R to target breast cancer in nude mice. Anticancer Res. 2012;32:2501-2508. PMID:22753706
[47] Zhang Y, Miwa S, Zhang N, et al. Tumor-targeting Salmonella typhimurium A1-R arrests growth of breast-cancer brain metastasis. Oncotarget. 2015;6:2615-2622. PMID:25575815
[48] Uchugonova A, Zhao M, Zhang Y, et al. Cancer-cell killing by engineered Salmonella imaged by multiphoton tomography in live mice. Anticancer Res. 2012;32:4331-4337. PMID:23060555
[49] Liu F, Zhang L, Hoffman RM, et al. Vessel destruction by tumor-targeting Salmonella typhimurium A1-R is enhanced by high tumor vascularity. Cell Cycle. 2010;9:4518-4524. 10.4161/cc.9.22.13744. PMID:21135579
[50] Nagakura C, Hayashi K, Zhao M, et al. Efficacy of a genetically-modified Salmonella typhimurium in an orthotopic human pancreatic cancer in nude mice. Anticancer Res. 2009;29:1873-1378. PMID:19528442
[51] Yam C, Zhao M, Hayashi K, et al. Monotherapy with a tumor-targeting mutant of S. typhimurium inhibits liver metastasis in a mouse model of pancreatic cancer. J Surg Res. 2010;164:248-255. 10.1016/j.jss.2009.02.023. PMID:19766244
[52] Hiroshima Y, Zhao M, Zhang Y, et al. Comparison of efficacy of Salmonella typhimurium A1-R and chemotherapy on stem-like and non-stem human pancreatic cancer cells. Cell Cycle. 2013;12:2774-2780. 10.4161/cc.25872. PMID:23966167
[53] Hiroshima Y, Zhao M, Maawy A, et al. Efficacy of Salmonella typhimurium A1-R versus chemotherapy on a pancreatic cancer patient-derived orthotopic xenograft (PDOX). J Cell Biochem. 2014;115:1254-1261. 10.1002/jcb.24769. PMID:24435915
[54] Matsumoto Y, Miwa S, Zhang Y, et al. Efficacy of tumor-targeting Salmonella typhimurium A1-R on nude mouse models of metastatic and disseminated human ovarian cancer. J Cell Biochem. 2014;115:1996-2003. PMID:24924355
[55] Matsumoto Y, Miwa S, Zhang Y, et al. Intraperitoneal administration of tumor-targeting Salmonella typhimurium A1-R inhibits disseminated human ovarian cancer and extends survival in nude mice. Oncotarget. 2015;6:11369-11377. 10.18632/oncotarget.3607. PMID:25957417
[56] Yano S, Zhang Y, Zhao M, et al. Tumor-targeting Salmonella typhimurium A1-R decoys quiescent cancer cells to cycle as visualized by FUCCI imaging and become sensitive to chemotherapy. Cell Cycle. 2014;13:3958-3963. 10.4161/15384101.2014.964115. PMID:25483077
[57] Hiroshima Y, Zhang Y, Zhao M, et al. Tumor-targeting Salmonella typhimurium A1-R in combination with Trastuzumab eradicates HER-2-positive cervical cancer cells in patient-derived mouse models. PLoS One. 2015;10:e0120358. 10.1371/journal.pone.0120358. PMID:26047477
[58] Momiyama M, Zhao M, Kimura H, et al. Inhibition and eradication of human glioma with tumor-targeting Salmonella typhimurium in an orthotopic nude-mouse model. Cell Cycle. 2012;11:628-632. 10.4161/cc.11.3.19116. PMID:22274398
[59] Kimura H, Zhang L, Zhao M, et al. Targeted therapy of spinal cord glioma with a genetically-modified Salmonella typhimurium. Cell Proliferation. 2010;43:41-48. 10.1111/j.1365-2184.2009.00652.x. PMID:19922490
[60] Hiroshima Y, Zhao M, Zhang Y, et al. Tumor-targeting Salmonella typhimurium A1-R arrests a chemo-resistant patient soft-tissue sarcoma in nude mice. PLoS One. 2015;10:e0134324. 10.1371/journal.pone.0134324. PMID:26237416
[61] Hayashi K, Zhao M, Yamauchi K, et al. Cancer metastasis directly eradicated by targeted therapy with a modified Salmonella typhimurium. J Cell Biochem. 2009;106:992-998. 10.1002/jcb.22078. PMID:19199339
[62] Hayashi K, Zhao M, Yamauchi K, et al. Systemic targeting of primary bone tumor and lung metastasis of high-grade osteosarcoma in nude mice with a tumor-selective strain of Salmonella typhimurium. Cell Cycle. 2009;8:870-875. 10.4161/cc.8.6.7891. PMID:19221501
[63] Miwa S, Zhang Y, Baek K-E, et al.: Inhibition of spontaneous and experimental lung metastasis of soft-tissue sarcoma by tumor-targeting Salmonella typhimurium A1-R. Oncotarget. 2014;5:12849-12861. PMID:25528763
[64] Yano S, Li S, Han Q, et al. Selective methioninase-induced trap of cancer cells in S/G_2 phase visualized by FUCCI imaging confers chemosensitivity. Oncotarget. 2014;5:8729-8736. 10.18632/oncotarget.2369. PMID: 25238266
[65] Hoffman RM. Altered methionine metabolism, DNA methylation and oncogene expression in carcinogenesis: a review and synthesis. Biochim Biophys Acta Rev Cancer. 1984;738:49-87. 10.1016/0304-419X(84)90019-2.
[66] Hoffman RM, Jacobsen SJ. Reversible growth arrest in simian virus 40-transformed human fibroblasts. Proc Natl Acad Sci USA. 1980;77:7306-7310. 10.1073/pnas.77.12.7306. PMID: 6261250
[67] Stern PH, Hoffman RM. Enhanced *in vitro* selective toxicity of chemotherapeutic agents for human cancer cells based on a metabolic defect. J Natl Cancer Inst. 1986;76:629-639. 10.1093/jnci/76.4.629. PMID: 3457200
[68] Hoffman RM, Erbe RW. High *in vivo* rates of methionine biosynthesis in transformed human and malignant rat cells auxotrophic for methionine. Proc Natl Acad Sci USA. 1976;73:1523-1527. 10.1073/pnas.73.5.1523. PMID: 179090
[69] Hoffman RM, Jacobsen SJ, Erbe RW. Reversion to methionine independence by malignant rat and SV40-transformed human fibroblasts. Biochem Biophys Res Commun. 1978;82:228-234. 10.1016/0006-291X(78)90600-9. PMID: 208554
[70] Hoffman RM, Jacobsen SJ, Erbe RW. Reversion to methionine independence in simian virus 40-transformed human and malignant rat fibroblasts is associated with altered ploidy and altered properties of transformation. Proc Natl Acad Sci USA. 1979;76:1313-1317. 10.1073/pnas.76.3.1313. PMID: 220612
[71] Coalson DW, Mecham JO, Stem PH, et al. Reduced availability of endogenously synthesized methionine for S-adenosylmethionine formation in methionine-dependent cancer cells. Proc Natl Acad Sci USA. 1982;79:4248-4251. 10.1073/pnas.79.14.4248. PMID: 6289297
[72] Stem PH, Mecham JO, Wallace CD, et al. Reduced free-methionine in methionine-dependent SV40-transformed human fibroblasts synthesizing apparently normal amounts of methionine. J Cell Physiol. 1983;117:9-14. 10.1002/jcp.1041170103. PMID: 6311851
[73] Mecham JO, Rowitch D, Wallace CD, et al. The metabolic defect of methionine dependence occurs frequently in human tumor cell lines. Biochem Biophys Res Commun. 1983;117:429-434. 10.1016/0006-291X(83)91218-4. PMID: 6661235
[74] Stern PH, Wallace CD, Hoffman RM. Altered methionine metabolism occurs in all members of a set of diverse human tumor cell lines. J Cell Physiol. 1984;119:29-34. 10.1002/jcp.1041190106. PMID: 6707100
[75] Stern PH, Hoffman RM. Elevated overall rates of transmethylation in cell lines from diverse human tumors. In Vitro. 1984;20:663-670. 10.1007/BF02619617. PMID: 6500606
[76] Tan Y, Xu M, Hoffman RM. Broad selective efficacy of recombinant methioninase and polyethylene glycol-modified recombinant methioninase on cancer cells *in vitro*. Anticancer Res. 2010;30:1041-1046. PMID: 20530407
[77] Tan Y, Xu M, Tan X-Z, et al. Overexpression and large-scale production of recombinant L-methionine-α-deamino-γ- mercaptomethanelyase for novel anticancer therapy. Prot Exp Purification. 1997;9:233-245. doi:10.1006/prep.1996.0700.
[78] Blagosklonny MV. Matching targets for selective cancer therapy. Drug Discov Today. 2003;8:1104-7. 10.1016/S1359-6446(03)02806-X. PMID: 14678733
[79] Blagosklonny MV. Teratogens as anti-cancer drugs. Cell Cycle. 2005;4:1518-21. 10.4161/cc.4.11.2208. PMID: 16258270

[80] Blagosklonny MV. Treatment with inhibitors of caspases, that are substrates of drug transporters, selectively permits chemotherapy-induced apoptosis in multidrug-resistant cells but protects normal cells. Leukemia. 2001;15:936-41. 10.1038/sj.leu.2402127. PMID: 11417480

[81] Blagosklonny MV. Target for cancer therapy: proliferating cells or stem cells. Leukemia. 2006;20:385-91. 10.1038/sj.leu.2404075. PMID: 16357832

[82] Apontes P, Leontieva OV, Demidenko ZN, et al. Exploring long-term protection of normal human fibroblasts and epithelial cells from chemotherapy in cell culture. Oncotarget. 2011;2:222-33. 10.18632/oncotarget.248. PMID: 21447859

[83] Blagosklonny MV. Tissue-selective therapy of cancer. Br J Cancer. 2003;89:1147-51. 10.1038/sj.bjc.6601256. PMID: 14520435